Structural control with tuned inertial mass electromagnetic transducers

Takehiko Asai[1*], Yoshikazu Araki[2] and Kohju Ikago[3]

[1] *Faculty of Engineering, Information and Systems, University of Tsukuba, Tsukuba, Ibaraki 305-8573, Japan*
[2] *Department of Architecture and Architectural Engineering, Kyoto University, Nishikyo, Kyoto 615-8540, Japan*
[3] *International Research Institute of Disaster Science, Tohoku University, Sendai, Miyagi 980-0845, Japan*

SUMMARY

This paper investigates the validity of the tuned inertial mass electromagnetic transducer (TIMET) applied to building structures subjected to seismic motions. The TIMET is a device inspired by two innovative structural control devices proposed recently, i.e., tuned viscous mass damper (TVMD) and electromagnetic transducer (ET). The TIMET consists of a spring, an inertial mass produced by a ball screw mechanism, and an ET part composed of a motor and an electrical circuit. The stiffness of the spring is tuned such that the inertial mass resonates with the vibrating building. This makes the motor installed in parallel with the inertial mass run up in an efficient way and the vibration energy is converted to electrical energy effectively. As a result, vibration of the building decays fast and electrical energy is stored. This generated energy is reusable for the self-powered control systems, structural health monitoring, emergency power source, and so on. In this paper, through numerical simulation studies employing the scaled three-story building model proposed for benchmark studies, the vibration reduction and energy harvesting capabilities of the TIMET is explored and the application potentiality to civil structures is discussed. Copyright © 2017 John Wiley & Sons, Ltd.

1. INTRODUCTION

Structural control technologies play a critical role to protect our lives and properties from severe natural disasters such as earthquakes and strong winds. To date, various kinds of structural control devices for civil structures have been proposed by many researchers and engineers [1]. One of the structural control strategies which already reached the mature stage is the tuned mass damper (TMD) [2]. The TMD is a dynamic vibration absorber, consisting of an auxiliary mass located at the top of the building and connected through a spring and damper. And the spring stiffness is tuned to absorb the input energy from external disturbances effectively and to reduce the amplitude of the building vibration. However, for practical reasons, the auxiliary mass is limited to on the order of several percent of the mass of the total structure. Thus this makes the TMD less effective for strong disturbances such as earthquake loadings.

To solve the problem of the limited auxiliary mass, various kinds of the structural control devices for civil structures with the *inerter* have been developed by many researchers including the tuned viscous mass damper (TVMD) [3], tuned inerter damper (TID) [4, 5], tuned mass damper inerter (TMDI) [6], and T tuned inerter damper (TTID) [7]. The inerter was introduced in [8] originally.

---

*Correspondence to: Faculty of Engineering, Information and Systems, University of Tsukuba, Tsukuba, Ibaraki 305-8573, Japan. E-mail: asai@kz.tsukuba.ac.jp

The force produced by the inerter is proportional to the relative acceleration between both ends and the amplified equivalent mass effect, i.e., *inertance*, is realized by a mechanism using the hydraulic [9], ball screw [3], or rack and pinion inerter [8, 10].

For example, the TVMD proposed in [3] is divided into two parts: a rotational mass damper and a supporting spring. The rotational mass damper part consists of a ball screw mechanism, a rotating mass, and a damper made of a viscous material. The ball screw mechanism is employed to convert translational motion to rotational behavior. Then a rotary inertial mass effect is produced by rotating the relatively small physical mass and an amplified equivalent mass effect, i.e., inertance, is obtained. The system which can produce the amplified equivalent mass up to on the order of thousandfold have been developed [11]. This makes it possible for the TVMD to realize relatively large mass ratio to the structure, which typical TMDs can not realize. At the same time the input energy is absorbed by the viscous material as heat. In this system, the inertance and the viscous damper are connected in parallel and the spring is arranged in series with them. The device is connected to the structure through the spring, thus the stiffness of the spring is tuned so that the rotational inertial mass resonates with the structure, which leads to improvements of the energy absorption efficiency and vibration mitigation performance [12, 13].

While as another structural control device, the electromagnetic transducer (ET) has been proposed in [14, 15]. This device is composed of a ball screw mechanism and a motor, thus in the same way as the TVMD, linear motion is changed to rotation which spins the motor through the ball screw mechanism. Then mechanical energy is converted into electrical energy with the motor and vibration decay is induced. In this case, the motor works as a generator. In addition, the motor can be used as an actuator and the multiple ETs can share the generated power. Thus the multiple ETs enable a self-powered control system by re-injecting the control force through a system called a Regenerative Force Actuation (RFA) Network [14, 16].

The authors have focused on the energy absorption capability of the TVMD, in which the inertance and damping part are arranged in parallel unlike the other tuned inerter devices, and the energy conversion system of the ET. Also, the fact that the ball screw mechanism is employed in both devices in common has attracted the authors' attention. Then by a combination of these two devices, tuned inertial mass electromagnetic transducers (TIMETs), which can increase energy generation efficiency, can be realized by one ball screw mechanism and have been proposed in the authors' previously published work [17]. In that paper, the authors showed the effectiveness of the proposed device on a single-degree-of-freedom (SDOF) oscillator as an energy harvester through numerical simulation studies.

The purpose of this paper is to asses not only the vibration reduction capability but also the energy harvesting efficiency of the TIMET on a building subjected to seismic motions. Because the external power grid is extremely unreliable during seismic events, the generated power is of value for the purpose of self-powered control system, structural health monitoring, emergency power source and so forth. In this paper, first, the mechanism of the TIMET and an SDOF oscillator model with the TIMET are reviewed briefly. And we introduce an effective TIMET configuration combined with the TMD system for building structures [18], in addition to the configuration where the TIMET are installed between two adjacent floors the same way as the TVMD proposed in literature [12]. Then the equation of motions are derived and the parameter design methods are introduced. Subsequently numerical simulation studies are implemented using the scaled three-story building model subjected to a disturbance created by the Kanai-Tajimi filter and three earthquake records. Conclusions obtained from this study then follow.

2. MODELS FOR TUNED INERTIAL MASS ELECTROMAGNETIC TRANSDUCERS

In this section, the mechanism of the TIMET proposed in [17] is reviewed briefly. First, the model of the TIMETs is introduced, and the equation of motion when the TIMET is installed on an SDOF oscillator is derived. Finally, the energy harvesting objective is defined.
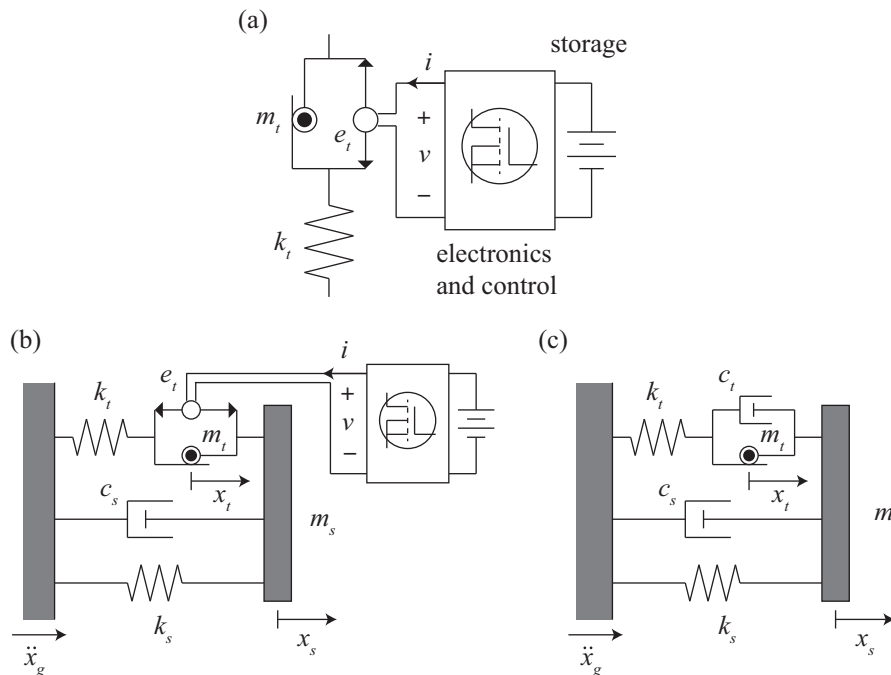
Figure 1. Schematic models: (a) TIMET, (b) SDOF oscillator with TIMET, and (c) Equivalent model of the SDOF oscillator with TIMET.

2.1. Tuned inertial mass electromagnetic transducer

The TIMET investigated in this research can be modeled as illustrated in Figure 1 (a). As can be seen, the TIMET consists of three parts: damping, inertial mass, and liner spring parts. To decay vibration induced by disturbance, ordinary dampers absorb vibration energy by converting into heat. While the TIMET provides damping by electromechanical coupling coefficient e_t through a transducer and converts mechanical energy into electrical energy. The value of e_t is defined by the magnetic field of the rotor and the lead of the ball screw mechanism. Then this generated energy can be stored for later use. In parallel with the motor, inertance m_t is installed. As the inerter is realized through a ball screw mechanism, huge equivalent mass effect can be obtained by relatively small physical mass. And the linear spring whose stiffness is k_t is installed in series with the damping and inertial mass. To improve energy absorbing efficiency and vibration mitigation performance, we need design the value of k_t and control the current into the transducer i appropriately.

2.2. SDOF oscillator with TIMET

The model of an SDOF oscillator with the TIMET is shown in Figure 1 (b) schematically. Let m_s, c_s, and k_s be the mass, damping, and stiffness of the SDOF oscillator, then the equation of motion including the TIMET is derived as follows. If x_s is the displacement relative to the ground of the SDOF oscillator and x_t is the deformation of the inerter of the TIMET, the equation of motion of the oscillator would be

$$m_s\ddot{x}_s + c_s\dot{x}_s + k_s x_s = -m_s\ddot{x}_g - f_t \tag{1}$$

where $\ddot{x}_g$ is the ground acceleration and the force from the supporting spring whose stiffness is k_t is given by

$$f_t = k_t(x_s - x_t) \tag{2}$$

while the equation of motion of the TIMET part becomes

$$m_t\ddot{x}_t = e_t i + f_t \tag{3}$$

Also the relationship between the current and voltage is defined as

$$i = -Yv \tag{4}$$

where Y is a time-invariant feedback gain, which can be adjusted by a MOSFET. Under this feedback law, the electrical load can be considered a resistor. Thus Y has units of admittance, so constant Y is called static admittance in this paper. And the voltage v can be expressed, from the back-EMF, as

$$v = e_t \dot{x}_t \tag{5}$$

Thus substituting Eq. (5) into Eq. (4) yields

$$i = -Y e_t \dot{x}_t \tag{6}$$

Hence Equation (3) can be rewritten, with respect to the velocity of the oscillator mass $\dot{x}_t$, as

$$m_t \ddot{x}_t + c_t \dot{x}_t = f_t \tag{7}$$

where

$$c_t = Y e_t^2 \tag{8}$$

Thus the model for the SDOF oscillator with the TIMET shown in Figure 1 (b) can be remodeled by using a dashpot whose damping is c_t as illustrated in Figure 1 (c). Therefore, by defining $\mathbf{x} = \begin{bmatrix} x_s & x_t \end{bmatrix}^T$, Equations (1) and (7) for the SDOF oscillator with the TIMET are expressed, in matrix form, as

$$\mathbf{M}\ddot{\mathbf{x}} + \mathbf{C}\dot{\mathbf{x}} + \mathbf{K}\mathbf{x} = -\mathbf{M}\boldsymbol{\Gamma}\ddot{x}_g \tag{9}$$

where

$$\mathbf{M} = \begin{bmatrix} m_s & 0 \\ 0 & m_t \end{bmatrix}, \qquad \mathbf{C} = \begin{bmatrix} c_s & 0 \\ 0 & c_t \end{bmatrix}, \qquad \mathbf{K} = \begin{bmatrix} k_s + k_t & -k_t \\ -k_t & k_t \end{bmatrix}, \qquad \boldsymbol{\Gamma} = \begin{bmatrix} 1 \\ 0 \end{bmatrix} \tag{10}$$

Note that hereafter in this paper, a dashpot is used to express the damping provided by TIMETs instead of an electromagnetic coupling coefficient and the electrical circuit.

2.3. Energy harvesting objective

To assess the energy harvesting potential for the proposed system, the power delivered to storage needs to be defined. As in [16, 19], the power delivered to storage is defined as the power extracted by the transducer minus the the transmission losses in the transducer and power electronic circuitry in this paper.

We have that the electromechanical transduction power $P_e(t)$ is preserved between mechanical and electrical sides of the transducers; i.e.,

$$P_e(t) = iv = -c_t \dot{x}_t^2 \tag{11}$$

with the convention that positive $P_e(t)$ implies energy flow from the electrical network to the mechanical system. While typically the expression for the transmission losses $P_d(t)$ is quite complicated because the transmission losses happens due to various causes on the electronic hardware. However, for the purpose of this paper, we assume simply that the transmission loss is resistive; i.e.,

$$P_d(t) = i^2 R = \frac{c_t^2 R}{e_t^2} \dot{x}_t^2 \tag{12}$$

where $R > 0$ is the transmission resistance. For example, if the losses were entirely comprised of coil losses in the transducers, then R is equal to the coil resistance. For more complex loss models, which incorporate MOSFET and diode conduction losses in the converters, past work has shown that these situations can also be conservatively approximated by a resistive loss term, together with a static power offset [20]. Defining $\bar{c}_t = e_t^2/R$, which is a positive value with units of viscous
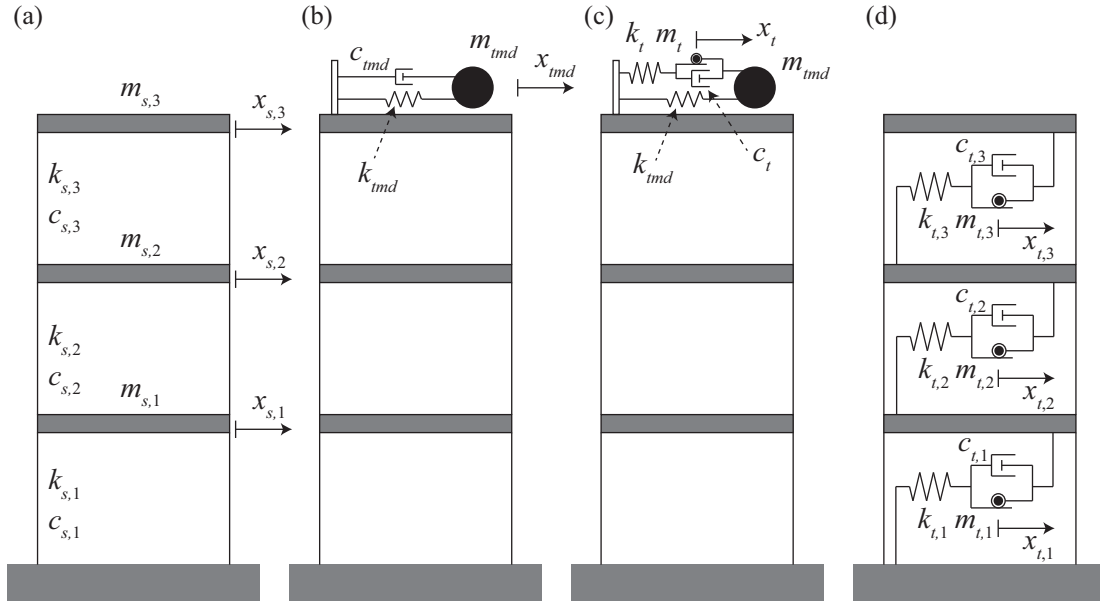
Figure 2. Building models: (a) Three-story building model, (b) TMD with ET, (c) TMD with TIMET, and (d) Interstory TIMET.

damping, gives

$$P_d(t) = \frac{c_t^2}{\bar{c}_t} \dot{x}_t^2 \tag{13}$$

and physically, $\bar{c}_t$ represents the supplemental viscous damping that would relate the velocity $\dot{x}_t$ to the output force $c_t \dot{x}_t$ if the coil of the transducer is shorted. Thus $\bar{c}_t$ is determined by the specification of the transducer and represents the maximum viscous damping the transducer can exert.

With the above definitions and assumptions, we can now define the power delivered to storage as

$$P_g(t) = -P_e(t) - P_l(t) = \left(c_t - \frac{c_t^2}{\bar{c}_t} \right) \dot{x}_t^2 \tag{14}$$

3. PROBLEM FORMULATION

To explore the possibilities of the TIMET on buildings subjected to seismic motions, a three-story shear building model illustrated in Figure 2 (a) is considered. For comparison, as shown in Figure 2 (b), a typical TMD employing an ET instead of viscous damper is investigated. In addition, two configurations of the TIMET for building structures are examined; one is a TMD with TIMET system, in which the TIMET mechanism is installed between the top floor and the auxiliary mass for the TMD as depicted in Figure 2 (c), and the other is an interstory TIMET system, in which the TIMETs are installed between floors as shown in Figure 2 (d). This is the typical configuration for the TVMD proposed in previous work [12]. In this section, the equations of motion of these systems are developed.

3.1. Building model

First of all, the equation of motion of the three-story shear building model shown in Figure 2 (a) is derived. Let $x_{s,j}$, $m_{s,j}$, $k_{s,j}$, $c_{s,j}$ be the translational displacement relative to the ground, mass, stiffness, and damping of the jth floor. Then the equation of motion can be expressed by

$$\mathbf{M}_s \ddot{\mathbf{x}}_s + \mathbf{C}_s \dot{\mathbf{x}}_s + \mathbf{K}_s \mathbf{x}_s = -\mathbf{M}_s \mathbf{\Gamma}_s \ddot{x}_g \tag{15}$$

where $\ddot{x}_g$ is the ground acceleration, the displacement vector $\mathbf{x}_s$ is defined as $\mathbf{x}_s = \begin{bmatrix} x_{s,1} & x_{s,2} & x_{s,3} \end{bmatrix}^T$, and the mass matrix $\mathbf{M}_s$, stiffness matrix $\mathbf{K}_s$, damping matrix $\mathbf{C}_s$, and influence vector $\mathbf{\Gamma}_s$ become:

$$\mathbf{M}_s = \begin{bmatrix} m_1 & 0 & 0 \\ 0 & m_2 & 0 \\ 0 & 0 & m_3 \end{bmatrix}, \quad \mathbf{K}_s = \begin{bmatrix} k_{s,1}+k_{s,2} & -k_{s,2} & 0 \\ -k_{s,2} & k_{s,2}+k_{s,3} & -k_{s,3} \\ 0 & -k_{s,3} & k_{s,3} \end{bmatrix},$$
$$\mathbf{C}_s = \begin{bmatrix} c_{s,1}+c_{s,2} & -c_{s,2} & 0 \\ -c_{s,2} & c_{s,2}+c_{s,3} & -c_{s,3} \\ 0 & -c_{s,3} & c_{s,3} \end{bmatrix}, \quad \mathbf{\Gamma}_s = \begin{bmatrix} 1 \\ 1 \\ 1 \end{bmatrix} \tag{16}$$

respectively.

3.2. TMD with ET

Next, the equation of motion of the three-story building employing the TMD with ET system shown in Figure 2 (b) is derived. Define the auxiliary mass, stiffness of the spring connecting the auxiliary mass to the third floor, and damping induced by the ET as m_{tmd}, k_{tmd}, and c_{tmd}, respectively. Then letting the relative displacement of the tuned mass be x_{tmd} and the displacement vector be $\mathbf{x} = \begin{bmatrix} \mathbf{x}_s^T & x_{tmd} \end{bmatrix}^T$ yields the equation of motion expressed as Equation (9) where the coefficient matrices are:

$$\mathbf{M} = \begin{bmatrix} \mathbf{M}_s & \mathbf{0} \\ \mathbf{0} & m_{tmd} \end{bmatrix}, \quad \mathbf{K} = \begin{bmatrix} k_{s,1}+k_{s,2} & -k_{s,2} & 0 & 0 \\ -k_{s,2} & k_{s,2}+k_{s,3} & -k_{s,3} & 0 \\ 0 & -k_{s,3} & k_{s,3}+k_{tmd} & -k_{tmd} \\ 0 & 0 & -k_{tmd} & k_{tmd} \end{bmatrix},$$
$$\mathbf{C} = \begin{bmatrix} c_{s,1}+c_{s,2} & -c_{s,2} & 0 & 0 \\ -c_{s,2} & c_{s,2}+c_{s,3} & -c_{s,3} & 0 \\ 0 & -c_{s,3} & c_{s,3}+c_{tmd} & -c_{tmd} \\ 0 & 0 & -c_{tmd} & c_{tmd} \end{bmatrix}, \quad \mathbf{\Gamma} = \begin{bmatrix} \mathbf{\Gamma}_s \\ 1 \end{bmatrix} \tag{17}$$

3.3. TMD with TIMET

In a similar way, $\mathbf{M}$, $\mathbf{C}$, $\mathbf{K}$, and $\mathbf{\Gamma}$ matrices for the TMD with TIMET illustrated in Figure 2 (c) are developed. Define the equivalent mass, supporting spring stiffness, damping for the TIMET be m_t, k_t, and c_t, and let the deformation of the inerter be x_t and the displacement vector be $\mathbf{x} = \begin{bmatrix} \mathbf{x}_s^T & x_{tmd} & x_t \end{bmatrix}^T$. Then by referring to the SDOF oscillator case given as Equation (10), the matrices for the equation of motion of form Equation (9) can be derived as follows:

$$\mathbf{M} = \begin{bmatrix} \mathbf{M}_s & \mathbf{0} & \mathbf{0} \\ \mathbf{0} & m_{tmd} & 0 \\ \mathbf{0} & 0 & m_t \end{bmatrix},$$
$$\mathbf{K} = \begin{bmatrix} k_{s,1}+k_{s,2} & -k_{s,2} & 0 & 0 & 0 \\ -k_{s,2} & k_{s,2}+k_{s,3} & -k_{s,3} & 0 & 0 \\ 0 & -k_{s,3} & k_{s,3}+k_{tmd}+k_t & -k_{tmd}-k_t & k_t \\ 0 & 0 & -k_{tmd}-k_t & k_{tmd}+k_t & -k_t \\ 0 & 0 & k_t & -k_t & k_t \end{bmatrix},$$
$$\mathbf{C} = \begin{bmatrix} c_{s,1}+c_{s,2} & -c_{s,2} & 0 & 0 & 0 \\ -c_{s,2} & c_{s,2}+c_{s,3} & -c_{s,3} & 0 & 0 \\ 0 & -c_{s,3} & c_{s,3}+c_{tmd} & -c_{tmd} & 0 \\ 0 & 0 & -c_{tmd} & c_{tmd} & 0 \\ 0 & 0 & 0 & 0 & c_t \end{bmatrix}, \quad \mathbf{\Gamma} = \begin{bmatrix} \mathbf{\Gamma}_s \\ 1 \\ 0 \end{bmatrix} \tag{18}$$

3.4. Interstory TIMET

Finally, the equation of motion for the interstory TIMET configuration depicted in Figure 2 (d) is developed. Assuming that the equivalent mass, supporting spring stiffness, and damping for the TIMET installed of the jth floor are $m_{t,j}$, $k_{t,j}$, and $c_{t,j}$, respectively. In addition, let the deformation of the inerter of the jth TIMET be $x_{t,j}$ and $\mathbf{x}_t = \begin{bmatrix} x_{t,1} & x_{t,2} & x_{t,3} \end{bmatrix}^T$. Then defining $\mathbf{x} = \begin{bmatrix} \mathbf{x}_s^T & \mathbf{x}_t^T \end{bmatrix}^T$, the coefficient matrices for the equation given as Equation (9) are derived as:

$$\mathbf{M} = \begin{bmatrix} \mathbf{M}_s & \mathbf{0} \\ \mathbf{0} & \mathbf{M}_t \end{bmatrix}, \quad \mathbf{M}_t = \begin{bmatrix} m_{t,1} & 0 & 0 \\ 0 & m_{t,2} & 0 \\ 0 & 0 & m_{t,3} \end{bmatrix},$$

$$\mathbf{K} = \begin{bmatrix} k_{s,1}+k_{s,2}+k_{t,1}+k_{t,2} & -k_{s,2}-k_{t,2} & 0 & -k_{t,1} & k_{t,2} & 0 \\ -k_{s,2}-k_{t,2} & k_{s,2}+k_{s,3}+k_{t,2}+k_{t,3} & -k_{s,3}-k_{t,3} & 0 & -k_{t,2} & k_{t,3} \\ 0 & -k_{s,3}-k_{t,3} & k_{s,3}+k_{t,3} & 0 & 0 & -k_{t,3} \\ -k_{t,1} & 0 & 0 & k_{t,1} & 0 & 0 \\ k_{t,2} & -k_{t,2} & 0 & 0 & k_{t,2} & 0 \\ 0 & k_{t,3} & -k_{t,3} & 0 & 0 & k_{t,3} \end{bmatrix},$$

$$\mathbf{C} = \begin{bmatrix} \mathbf{C}_s & \mathbf{0} \\ \mathbf{0} & \mathbf{C}_t \end{bmatrix}, \quad \mathbf{C}_t = \begin{bmatrix} c_{t,1} & 0 & 0 \\ 0 & c_{t,2} & 0 \\ 0 & 0 & c_{t,3} \end{bmatrix}, \quad \mathbf{\Gamma} = \begin{bmatrix} \mathbf{\Gamma}_s \\ \mathbf{0} \end{bmatrix}$$

$$(19)$$

4. PARAMETER DESIGN

In this section, the parameter design methods for the systems developed in the previous section are explained.

4.1. TMD with ET

The TMD with ET can be considered as a typical TMD system except for the energy conversion manner. Thus the stiffness and damping for this system are determined, based on the method proposed for the TMD by Den Hartog [2], as

$$k_{tmd} = (\beta_{tmd}\omega_r)^2 m_{tmd} \tag{20}$$

$$c_{tmd} = 2\zeta_{tmd}\beta_{tmd}\omega_r m_{tmd} \tag{21}$$

where ω_r is the natural frequency of the rth mode of the building and β_{tmd} and ζ_{tmd} for the rth mode are given by

$$\beta_{tmd} = \frac{1}{1+\mu_{tmd}}, \quad \zeta_{tmd} = \sqrt{\frac{3\mu_{tmd}}{8(1+\mu_{tmd})}} \tag{22}$$

And the mass ratio μ_{tmd} for the rth mode is defined as

$$\mu_{tmd} = \frac{\bar{M}_{tmd,r}}{\bar{M}_{s,r}} \tag{23}$$

where $\bar{M}_{s,r}$ is the rth modal mass of the building defined, with the rth mode shape vector $\mathbf{u}_r = \begin{bmatrix} u_{r,1} & u_{r,2} & u_{r,3} \end{bmatrix}^T$, as

$$\bar{M}_{s,r} = \sum_{j=1}^{3} m_j u_{r,j}^2 \tag{24}$$

and $\bar{M}_{tmd,r}$ is the rth modal mass of the TMD placed on the 3rd floor and is given by

$$\bar{M}_{tmd,r} = m_{tmd} u_{r,3}^2 \tag{25}$$

4.2. TMD with TIMET

To determine the values for k_t and c_t for the TMD with TIMET system, these parameters are treated as control gains for a stochastic optimal control problem subjected to a white noise input and the optimized values are sought through the algorithms presented in [21, 17].

By seeing the forces applied by the transducer and supporting spring of the TIMET as the control forces to the system, the equation of motion given by Equations (9) and (18) can be rewritten as

$$\hat{\mathbf{M}}\ddot{\mathbf{x}} + \hat{\mathbf{C}}\dot{\mathbf{x}} + \hat{\mathbf{K}}\mathbf{x} = \hat{\mathbf{E}}f_i + \hat{\mathbf{F}}f_s - \hat{\mathbf{M}}\hat{\mathbf{\Gamma}}\ddot{x}_g \tag{26}$$

where

$$\hat{\mathbf{M}} = \mathbf{M}, \quad \hat{\mathbf{\Gamma}} = \mathbf{\Gamma}, \quad \hat{\mathbf{K}} = \begin{bmatrix} k_{s,1} + k_{s,2} & -k_{s,2} & 0 & 0 & 0 \\ -k_{s,2} & k_{s,2} + k_{s,3} & -k_{s,3} & 0 & 0 \\ 0 & -k_{s,3} & k_{s,3} + k_{tmd} & -k_{tmd} & 0 \\ 0 & 0 & -k_{tmd} & k_{tmd} & 0 \\ 0 & 0 & 0 & 0 & 0 \end{bmatrix}$$

$$\hat{\mathbf{C}} = \begin{bmatrix} c_{s,1} + c_{s,2} & -c_{s,2} & 0 & 0 & 0 \\ -c_{s,2} & c_{s,2} + c_{s,3} & -c_{s,3} & 0 & 0 \\ 0 & -c_{s,3} & c_{s,3} + c_{tmd} & -c_{tmd} & 0 \\ 0 & 0 & -c_{tmd} & c_{tmd} & 0 \\ 0 & 0 & 0 & 0 & 0 \end{bmatrix}, \quad \hat{\mathbf{E}} = \begin{bmatrix} 0 \\ 0 \\ 0 \\ 0 \\ 1 \end{bmatrix}, \quad \hat{\mathbf{F}} = \begin{bmatrix} 0 \\ 0 \\ 1 \\ -1 \\ 1 \end{bmatrix} \tag{27}$$

and f_i and f_s are the forces by the transducer and the spring defined by

$$f_i = -c_t\dot{x}_t, \quad f_s = k_t(x_{tmd} - x_{s,3} - x_t) \tag{28}$$

respectively.

The equation of motion given as Equation (26) can be expressed as the state-space representation of the form

$$\dot{\mathbf{z}}_t = \mathbf{A}_t\mathbf{z}_t + \mathbf{B}_{ti}f_i + \mathbf{B}_{ts}f_s + \mathbf{G}_t\ddot{x}_g \tag{29}$$

where the state vector is $\mathbf{z}_t = \begin{bmatrix} \mathbf{x}^T & \dot{\mathbf{x}}^T \end{bmatrix}^T$ and $\mathbf{A}_t$, $\mathbf{B}_{ti}$, $\mathbf{B}_{ts}$, and $\mathbf{G}_t$ matrices are:

$$\mathbf{A}_t = \begin{bmatrix} \mathbf{0} & \mathbf{I} \\ -\hat{\mathbf{M}}^{-1}\hat{\mathbf{K}} & -\hat{\mathbf{M}}^{-1}\hat{\mathbf{C}} \end{bmatrix}, \quad \mathbf{B}_{ti} = \begin{bmatrix} \mathbf{0} \\ -\hat{\mathbf{M}}^{-1}\hat{\mathbf{E}} \end{bmatrix}, \quad \mathbf{B}_{ts} = \begin{bmatrix} \mathbf{0} \\ -\hat{\mathbf{M}}^{-1}\hat{\mathbf{F}} \end{bmatrix}, \quad \mathbf{G}_t = \begin{bmatrix} \mathbf{0} \\ -\hat{\mathbf{\Gamma}} \end{bmatrix} \tag{30}$$

Next, to apply the stochastic optimal control theory, the earthquake acceleration $\ddot{x}_g$ is modeled using a second-order noise filter called Kanai-Tajimi earthquake model [22] developed as

$$\dot{\mathbf{z}}_g = \mathbf{A}_g\mathbf{z}_g + \mathbf{B}_g w \tag{31}$$

$$\ddot{x}_g = \mathbf{C}_g\mathbf{z}_g \tag{32}$$

where

$$\mathbf{A}_g = \begin{bmatrix} 0 & 1 \\ -\omega_g^2 & -2\zeta_g\omega_g \end{bmatrix}, \quad \mathbf{B}_g = \begin{bmatrix} 0 \\ 1 \end{bmatrix}, \quad \mathbf{C}_g = \begin{bmatrix} \omega_g^2 & 2\zeta_g\omega_g \end{bmatrix} \tag{33}$$

and the exogenous input ω is assumed to be white noise with spectral intensity $\Phi_\omega = 1$.

Then defining $\mathbf{z} = \begin{bmatrix} \mathbf{z}_t^T & \mathbf{z}_g^T \end{bmatrix}^T$ leads to the augmented system given as

$$\dot{\mathbf{z}} = \mathbf{A}\mathbf{z} + \mathbf{B}_i f_i + \mathbf{B}_s f_s + \mathbf{G}w \tag{34}$$

where

$$\mathbf{A} = \begin{bmatrix} \mathbf{A}_t & \mathbf{G}_t\mathbf{C}_g \\ \mathbf{0} & \mathbf{A}_g \end{bmatrix}, \quad \mathbf{B}_i = \begin{bmatrix} \mathbf{B}_{ti} \\ \mathbf{0} \end{bmatrix}, \quad \mathbf{B}_s = \begin{bmatrix} \mathbf{B}_{ts} \\ \mathbf{0} \end{bmatrix}, \quad \mathbf{G} = \begin{bmatrix} \mathbf{0} \\ \mathbf{B}_g \end{bmatrix} \tag{35}$$

and the control forces given by Equation (28) are expressed, with the state $\mathbf{z}$, as

$$f_i = -c_t\mathbf{C}_i\mathbf{z}, \quad f_s = k_t\mathbf{C}_s\mathbf{z} \tag{36}$$

Then the closed form of the augmented state-space representation given by Equation (34) is derived as

$$\dot{\mathbf{z}} = (\mathbf{A} - \mathbf{B}_i c_t \mathbf{C}_i + \mathbf{B}_s k_t \mathbf{C}_s)\mathbf{z} + \mathbf{G}w \tag{37}$$

In this paper, to seek the optimal values for k_t and c_t, two objective functions are defined; one is the expectation of the square of the 3rd floor displacement $\mathcal{E}\, x_{s,3}^2$ and the other is the expectation of the generated power $\mathcal{E}\, P_g$. Since the 3rd floor distance is expressed as

$$x_{s,3} = \mathbf{C}_d \mathbf{z} \tag{38}$$

with appropriate $\mathbf{C}_d$, thus the expectation of the square would be

$$\mathcal{E}\, x_{s,3}^2 = \mathcal{E}(\mathbf{z}^T \mathbf{C}_d^T \mathbf{C}_d \mathbf{z}) = \mathbf{G}^T \mathbf{S}_d \mathbf{G} \tag{39}$$

where $\mathbf{S}_d = \mathbf{S}_d^T > 0$ is the solution to the Lyapunov equation [23]

$$(\mathbf{A} - \mathbf{B}_i c_t \mathbf{C}_i + \mathbf{B}_s k_t \mathbf{C}_s)^T \mathbf{S}_d + \mathbf{S}_d(\mathbf{A} - \mathbf{B}_i c_t \mathbf{C}_i + \mathbf{B}_s k_t \mathbf{C}_s) + \mathbf{C}_d \mathbf{C}_d^T = \mathbf{0} \tag{40}$$

Also, the velocity of the TIMET can be expressed as

$$\dot{x}_t = \mathbf{C}_i \mathbf{z} \tag{41}$$

thus from Equation (14), the expected power generation would be

$$\mathcal{E}\, P_g = \mathcal{E}\left(\mathbf{C}_i^T \left(c_t - \frac{c_t^2}{\bar{c}_t} \right) \mathbf{C}_i^T \right) = \mathbf{G}^T \mathbf{S}_p \mathbf{G} \tag{42}$$

where $\mathbf{S}_p = \mathbf{S}_p^T > 0$ is the solution to the Lyapunov equation

$$(\mathbf{A} - \mathbf{B}_i c_t \mathbf{C}_i + \mathbf{B}_f k_t \mathbf{C}_s)^T \mathbf{S}_p + \mathbf{S}_p(\mathbf{A} - \mathbf{B}_i c_t \mathbf{C}_i + \mathbf{B}_f k_t \mathbf{C}_s) + \mathbf{C}_i^T \left(c_t - \frac{c_t^2}{\bar{c}_t} \right) \mathbf{C}_i^T = \mathbf{0} \tag{43}$$

Therefore these parameter design problems are reduced to optimization problems to seek for the values for k_t and c_t to minimize Equation (39) subject to Equation (40) and to maximize Equation (42) subject to Equation (43). These values can be obtained employing convex over-bounding techniques, as originally proposed by [24, 25]. We will not delve into the details of these techniques here, but instead refer to [26], which outline the method in detail.

4.3. Interstory TIMET

In this paper, the parameters for the interstory TIMET system are designed by the method proposed for the TVMD in [12]. For these systems, the mass ratio for the rth mode is defined as

$$\mu_{it} = \frac{\bar{M}_{t,r}}{\bar{M}_{s,r}} \tag{44}$$

where the rth modal mass is defined by the same way as Equation (24) and the rth modal mass of the interstory TIMET is defined, with the rth mode shape vector $\mathbf{u}_r$ as

$$\bar{M}_{t,r} = m_{t,1} u_{r,1}^2 + \sum_{j=2}^{3} m_{t,j}(u_{r,j} - u_{r,j-1})^2 \tag{45}$$

because the TIMETs are installed between adjacent floors. Then we assume that the modal equivalent masses $m_{t,1}$, $m_{t,2}$, and $m_{t,3}$ are distributed in proportion to the stiffness of the building model, i.e., $k_{s,1}$, $k_{s,2}$, and $k_{s,3}$, then the equivalent mass of the TIMETs are obtained, with a constant value

$$c_m = \mu_{it} \frac{\sum_{j=1}^{3} m u_{r,j}^2}{u_{r,1}^2 + \sum_{j=2}^{3} k_i(u_{r,j} - u_{r,j-1})^2/k_1} \tag{46}$$

Table I. Parameters for the small-scale three-story benchmark building model

Mass (kg)		Stiffness (kN/m)		Damping (Ns/m)	
m_1	98.3	k_1	516	c_1	125
m_2	98.3	k_2	684	c_2	50
m_3	98.3	k_3	684	c_3	50

as

$$m_{t,j} = \frac{k_j}{k_1} c_m \quad \text{or} \quad m_{t,j} = \frac{\mu_t}{\omega_r^2} k_{s,j} \tag{47}$$

Also, the stiffness and equivalent damping for the jth TIMET are given by

$$k_{t,j} = (\beta_t \omega_r)^2 m_{t,j} \tag{48}$$

$$c_{t,j} = 2\zeta_t \beta_t \omega_r m_{t,j} \tag{49}$$

where β_t and ζ_t for the system tuned to the rth mode are defined as

$$\beta_t = \frac{1 - \sqrt{1 - 4\mu_{it}}}{2\mu_{it}}, \quad \zeta_t = \frac{\sqrt{3(1 - \sqrt{1 - 4\mu_{it}})}}{4} \tag{50}$$

The details for this design method can be found in [12].

5. NUMERICAL SIMULATION

To evaluate the effectiveness of the TIMET on a building structure subjected to earthquake loadings in terms of vibration mitigation and energy harvesting capability, numerical simulation studies are carried out in this section. The model used in this paper is the scaled lightly damped three-story building, which was previously investigated for various structural control strategies by many researchers [27, 28, 29, 30]. The parameter for this model is summarized in Table I. The natural frequencies are 5.44, 15.81, and 23.63Hz and the time scale factor is 0.2, making the natural frequencies of the model five times those of the prototype.

5.1. Parameters for the control devices

The parameters for the control devices are determined based on the methods introduced in the previous section here.

To design the TMD with ET, five mass ratios including 0.02 (case I), 0.03 (case II), 0.04 (case III), 0.05 (case IV), and 0.1 (case V), are set for comparison. Then m_{tmd}, k_{tmd}, and c_{tmd} are calculated according to the previously introduced method tuning to the 1st mode of the building. The obtained values as shown in Table II. The mass ratio 0.1 of the case V is not practical for typical TMD systems, however the case V is implemented for the purpose of comparison with the case I of the interstory TIMET with 0.1 mass ratio. And for $\bar{c}_{tmd}$, the same value used for the TMD on the same scaled building model given in [29] is chosen.

For the TMD with TIMET, the same values for m_{tmd} and k_{tmd} as for the mass ratio 0.04 of the case III of the TMD with ET system are used. The mass ratio μ_{tt}, which is defined as the ratio of m_t to m_{tmd}, is set to 0.02 (case I). 0.05 (case II), 0.1 (case III) and 0.15 (case IV). To design the controller, we assume the stationary random process created by the Kanai-Tajimi filter with $\omega_g = 15.4$ rad/s and $\zeta_g = 0.64$. In [31], it was shown that these values resemble a realistic earthquake spectrum. To reflect the time scaling of the structural model, $\omega_g = 15.4 \times 5 = 77$ rad/s is used instead. In Table III, the parameter values for the controllers obtained from the algorithm to reduce the 3rd floor displacement are denoted by D, while the values determined such that the power generation is maximized are denoted by P. Note that the value of $\bar{c}_t$ is assumed to be the same as $\bar{c}_{tmd}$.

Table II. Parameters for the TMD with ET configuration

	I	II	III	IV	V
μ_{tmd}	0.02	0.03	0.04	0.05	0.1
m_{tmd} (kg)	3.87	5.80	7.74	9.67	19.34
k_{tmd} (kN/m)	4.34	6.39	8.36	10.25	18.67
c_{tmd} (Ns/m)	22.23	40.25	61.07	84.13	221.92
$\bar{c}_{tmd}$ (Ns/m)	1160	1160	1160	1160	1160

Table III. Parameters for the TMD with TIMET configuration

	I-D	I-P	II-D	II-P	III-D	III-P	IV-D	IV-P
m_{tmd} (kg)	7.74	7.74	7.74	7.74	7.74	7.74	7.74	7.74
k_{tmd} (kN/m)	8.36	8.36	8.36	8.36	8.36	8.36	8.36	8.36
μ_{tt}	0.02	0.02	0.05	0.05	0.1	0.1	0.15	0.15
m_t (kg)	0.15	0.15	0.39	0.39	0.77	0.77	1.16	1.16
k_t (kN/m)	1.10	5.46	0.47	0.47	1.07	0.97	1.92	1.42
c_t (Ns/m)	49.75	32.20	3.27	3.23	13.56	10.43	30.56	18.47
$\bar{c}_t$ (Ns/m)	1160	1160	1160	1160	1160	1160	1160	1160

Table IV. Parameters for the interstory TIMET configuration

	I	II
μ_{it}	0.1	0.15
$m_{t,1}$	44.17 kg	66.25 kg
$m_{t,2}, m_{t,3}$	58.55 kg	87.82 kg
$k_{t,1}$	65.54 kNs/m	116.18 kNs/m
$k_{t,2}, k_{t,3}$	86.88 kNs/m	154. 00 kNs/m
$c_{t,1}$	699.5 Ns/m	1456.6 Ns/m
$c_{t,2}, c_{t,3}$	927.3 Ns/m	1930.8 Ns/m
$\bar{c}_{t,1}, \bar{c}_{t,2}, \bar{c}_{t,3}$	236 kNs/m	236 kNs/m

As mentioned in the previous section, the parameters for the interstory TIMET are determined based on the method proposed for the TVMD in [12]. The mass ratio is assumed to be 0.1(case I) and 0.15 (case II) because due to the rotary inertial mass effect, a relatively high values can be applicable for the mass ratio for the interstory TIMET without installing huge actual masses. For this system, the TIMET are tuned to the 1st mode as well as the TIMET with ET cases. The calculated values are summarized in Table IV. The values for $\bar{c}_{t,1}, \bar{c}_{t,2}, \bar{c}_{t,3}$ are referred to the model used in [29] as well.

5.2. Kanai-Tajimi filter

Now we investigate the responses to a stationary random process with a spectral density defined by the Kanai-Tajimi filter expressed by the state-space representation defined as Equations (31) and (32). The input excitation is the same as one used for designing the TMD with TIMET system, i.e., $\omega_g = 15.4 \times 5 = 77$ rad/s and $\zeta_g = 0.64$ except for the spectral intensity. For the input excitation, the spectral intensity is adjusted such that the RMS values of the input acceleration takes a constant value of $\sigma_{\ddot{x}_g} = 0.12g$ with the gravitational acceleration g as used in [32], i.e.,

$$\mathbf{C}_g = \sqrt{2S_0\pi} \begin{bmatrix} \omega_g^2 & 2\zeta_g\omega_g \end{bmatrix} \tag{51}$$

where

$$S_0 = \frac{0.03\zeta_g}{\pi\omega_g(4\zeta_g^2 + 1)}g^2 \tag{52}$$

instead of $\mathbf{C}_g$ in Equation (33).

Table V provides the RMS values denoted by σ of the relative displacement and absolute acceleration of each floor and the expected power generation defined by Equation (14). Notice that the power generation for the interstory TIMET cases is the summation of power generated from the three transducers. The observations obtained are summarized as follows:

1. As the auxiliary mass of the TMD with ET systems increases, the vibration mitigation performance is improving. While, for the TIMET with ET system, the case II shows the best power generation efficiency. This is due to the discrepancies of the input energies from the external disturbance.

2. By comparing the case III of the TMD with ET and the TMD with TIMET systems, it is shown that the use of TIMET with an appropriate equivalent mass instead of ET can reduce the response displacements by almost 6% and improve the power generation by around 5% of the TMD systems without increasing the auxiliary mass. In particular, the case IV of the TMD with ET needs additional 1.94 kg mass to the case III, however, the same or better performances can be achieved in displacement reduction and power generation by the cases of II-D, II-P, III-D, III-P of the TMD with TIMET systems with only 0.39 kg and 0.77 kg additional equivalent mass effect. What is more is these additional equivalent mass effect can be realized with a much lighter physical mass due to the ball screw mechanism. When the mass ratios are increased to $\mu_{tt} = 0.15$, the vibration of the auxiliary mass of the TMD is reduced, though the vibration reduction performances of the building are deteriorated.

3. The results obtained from the case V of the TMD with ET and the case I of the interstory TIMET show that the latter system has advantages on vibration reduction, power generation, and required actual mass under the same mass ratio condition $\mu_{tmd} = \mu_{it} = 0.1$. These results also show the superiority of the TIMET. Moreover, the case II of the interstory TIMET shows better performances than the case I in both vibration reduction and power generation.

5.3. Earthquake records

For further investigation of the effectiveness of the TIMET, we input three earthquake records including the 1995 JMA-Kobe, 1940 El Centro, and 1952 Taft records. To satisfy the scaling law based on the similitude law for the small-scale building model, the earthquakes are reproduced at 5 times the recorded rate. The time histories of the employed earthquake records are shown in Figure 3.

In addition to the peak (denoted by p) and RMS (denoted by σ) values of relative displacement and absolute acceleration of each floor and the auxiliary mass on the top, the generated energy during the duration of time 0 to t_f defined as

$$E_g = \int_0^{t_f} P_g(t)dt \tag{53}$$

and the input energy from 0 to t_f defined as [33]

$$E_{in} = -\int_0^{t_f} \left(\sum_{j=1}^{3} m_j\ddot{x}_g\dot{x}_{s,j} + m_t\ddot{x}_g\dot{x}_t\right) dt \tag{54}$$

for the TMD with ET and TMD with TIMET systems and

$$E_{in} = -\int_0^{t_f} \sum_{j=1}^{3} m_j\ddot{x}_g\dot{x}_{s,j}dt \tag{55}$$

Table V. Results for the Kanai-Tajimi filter

| Response	TMD with ET					TMD with TIMET								Interstory TIMET	
	I	II	III	IV	V	I-D	I-P	II-D	II-P	III-D	III-P	IV-D	IV-P	I	II
σ_{d1} (mm)	1.316	1.202	1.126	1.071	0.917	1.116	1.163	1.071	1.071	1.075	1.084	1.134	1.165	0.836	0.717
σ_{d2} (mm)	2.051	1.869	1.751	1.666	1.432	1.734	1.806	1.649	1.650	1.658	1.673	1.757	1.809	1.279	1.098
σ_{d3} (mm)	2.480	2.266	2.126	2.025	1.752	2.106	2.191	2.004	2.005	2.021	2.038	2.141	2.206	1.544	1.323
σ_{dm} (mm)	11.627	8.920	7.443	6.503	4.456	8.219	9.989	9.882	9.874	7.986	7.715	7.082	6.986		
σ_{a1} (m/s^2)	3.110	2.972	2.853	2.747	2.333	2.870	2.959	3.079	3.079	3.066	3.071	3.082	3.100	2.752	2.446
σ_{a2} (m/s^2)	2.636	2.427	2.286	2.179	1.860	2.272	2.373	2.243	2.243	2.217	2.231	2.293	2.337	1.923	1.726
σ_{a3} (m/s^2)	3.606	3.360	3.183	3.042	2.578	3.246	3.342	3.261	3.262	3.285	3.305	3.394	3.449	2.808	2.495
σ_{am} (m/s^2)	12.823	9.580	7.794	6.645	4.071	8.359	10.284	10.159	10.152	7.984	7.691	6.858	6.624		
$\mathcal{E} P_g$ (W)	3.145	3.169	3.164	3.141	2.880	3.198	3.223	3.321	3.321	3.293	3.299	3.225	3.248	3.424	3.512
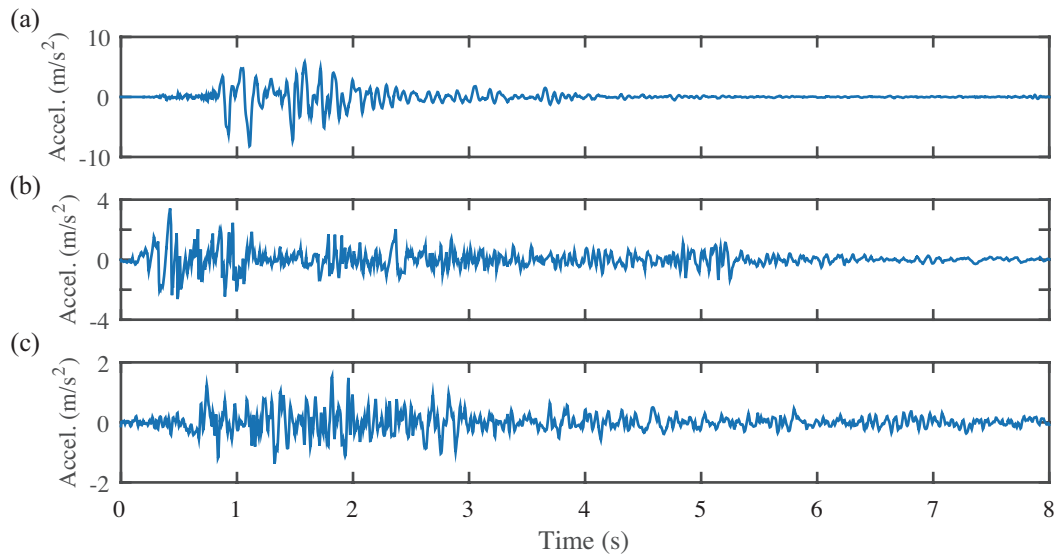
Figure 3. Input ground accelerations: (a) JMA Kobe, (b) El Centro, and (c) Taft.

for the interstory TIMET system, and we define the energy conversion ratio as E_g/E_{in}. The time histories of the 3rd floor displacements, generated powers, and input energies for the case III of the TMD with ET, the case III-D of the TMD with TIMET, and the case I of the interstory TIMET are plotted in Figures 4, 5, and 6, respectively. Also, the values obtained from the numerical simulations for all cases including the conversion ratios are summarized in Tables VI, VII, and VIII. The findings made from these simulations are:

1. Overall we can find similar trends as the Kanai-Tajimi spectrum cases about the vibration mitigation and energy harvesting capability.
2. Unlike the Kanai-Tajimi spectrum, the TMD with TIMET systems show response acceleration performances better than or comparable to the case III of the TMD with ET system to the earthquake records, especially in the RMS values. This is because the TIMET systems work well for the free vibration after the forced vibration.
3. Although the generated energies are affected by the input energies, the systems employing the TIMETs show more effective energy conversion ratios than the TMD with ET systems for the three input earthquake records.
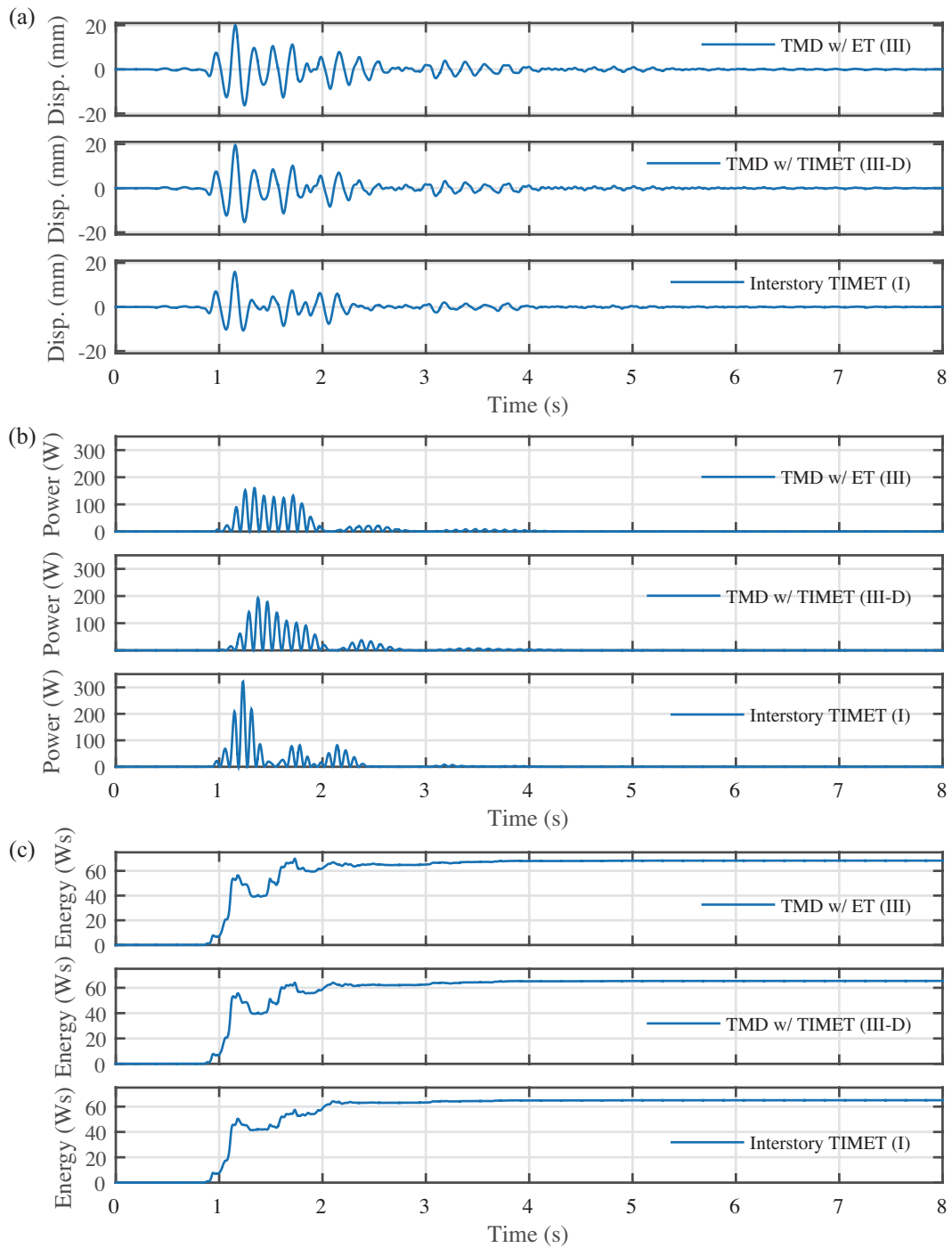
Figure 4. Time histories to JMA Kobe: (a) 3rd floor displacement, (b) Power generation, and (c) Input energy.
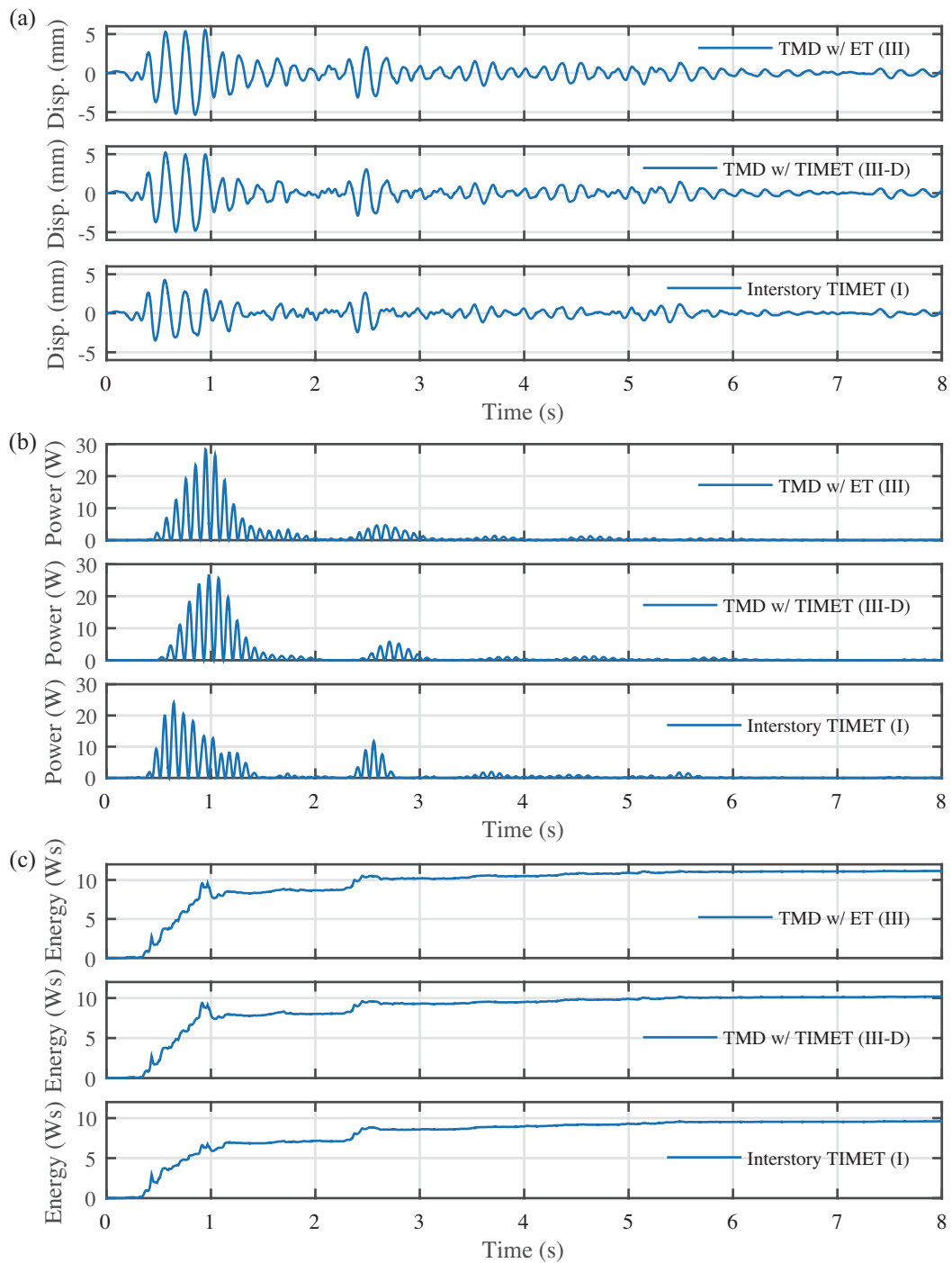
Figure 5. Time histories to El Centro: (a) 3rd floor displacement, (b) Power generation, and (c) Input energy.
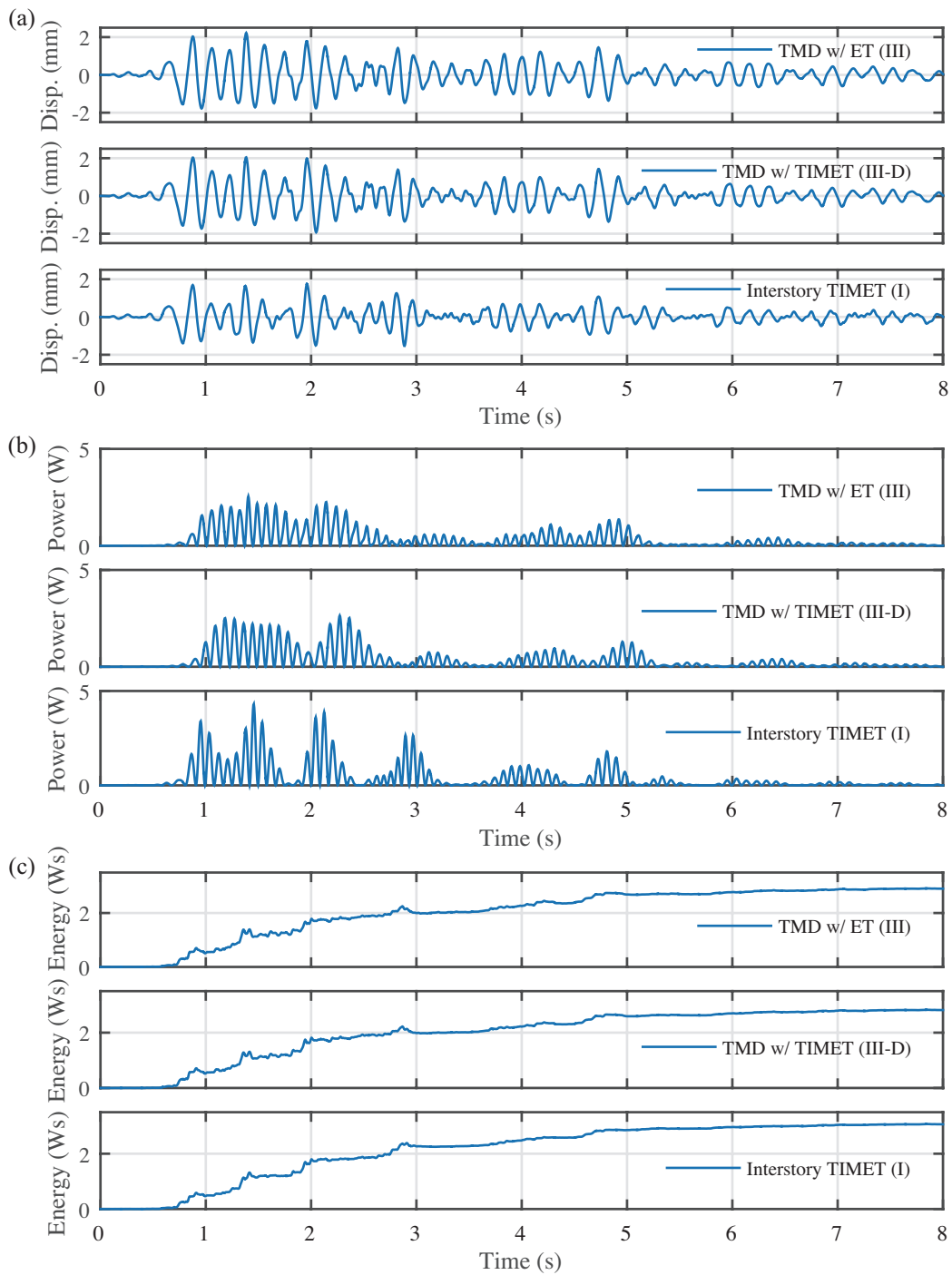
Figure 6. Time histories to Taft: (a) 3rd floor displacement, (b) Power generation, and (c) Input energy.

6. CONCLUSIONS

This paper investigates the possibilities of the TIMET on buildings structures subjected to seismic loadings from viewpoints of vibration mitigation and energy harvesting capability. The main contributions of this paper are as follows:

1. The configuration, in which the TIMET is combined with a TMD system, was investigated. Then, compared to the TMD with ET system, which is modeled as a traditional TMD, the effectiveness of the TMD with TIMET with an appropriate equivalent mass was shown through the numerical simulation studies. The advantages of the TMD with TIMET over the TMD with ET system are: (1) Vibration mitigation capability, (b) Energy harvesting efficiency, and (c) Less additional mass.
2. By examining the configurations of the TMD with TIMET and interstory TIMET, it was shown that the mechanism of the TIMET on the building model subjected to the Kanai-Tajimi spectrum and earthquake records worked well to improve the vibration reduction and power generation efficiency.
3. The relationship among the vibration responses, the input energy, and the absorbed energy of the building subjected to seismic motions was investigated. It was observed that even when the amount of input energy was small, the TIMET absorbed energy more effectively than the ET.
4. This paper showed that the ET including the TIMET mechanism has possibilities of taking the place of traditional dampers, which convert mechanical energy into heat energy and mitigate vibration in the field of seismic engineering. This is considered as a promising technology for structural control and health monitoring systems independent of the external power grid and for realizing sustainable societies and smart cities.

To improve the performance, the optimum placement of the TIMET considering not only vibration reduction and energy harvesting efficiency but also practical constraints such as cost should be explored, which is our future work.

REFERENCES

1. Housner GW, Bergman L, Caughey T, Chassiakos A, Claus R, Masri S, Skelton R, Soong T, Spencer BF Jr, Yao J. Structural control: Past, present, and future. *Journal of Engineering Mechanics* 1997; **123**(9):897–971.
2. Den Hartog JP. *Mechanical Vibrations*. Civil, Mechanical and Other Engineering Series, Dover Publications: New York, NY, 1985. URL https://books.google.co.jp/books?id=-Pu5YlgY4QsC.
3. Ikago K, Saito K, Inoue N. Seismic control of single-degree-of-freedom structure using tuned viscous mass damper. *Earthquake Engineering & Structural Dynamics* 2012; **41**(3):453–474, doi:10.1002/eqe.1138.
4. Lazar IF, Neild S, Wagg D. Using an inerter-based device for structural vibration suppression. *Earthquake Engineering & Structural Dynamics* 2014; **43**(8):1129–1147, doi:10.1002/eqe.2390. URL http://dx.doi.org/10.1002/eqe.2390.
5. Krenk S, Høgsberg J. Tuned resonant mass or inerter-based absorbers: unified calibration with quasi-dynamic flexibility and inertia correction. *Proceedings of the Royal Society of London A: Mathematical, Physical and Engineering Sciences* 2016; **472**(2185), doi:10.1098/rspa.2015.0718. URL http://rspa.royalsocietypublishing.org/content/472/2185/20150718.
6. Marian L, Giaralis A. Optimal design of a novel tuned mass-damper-inerter (TMDI) passive vibration control configuration for stochastically support-excited structural systems. *Probabilistic Engineering Mechanics* 2014; **38**:156 – 164, doi:https://doi.org/10.1016/j.probengmech.2014.03.007. URL http://www.sciencedirect.com/science/article/pii/S0266892014000216.
7. Zhang SY, Jiang JZ, Neild S. Optimal configurations for a linear vibration suppression device in a multi-storey building. *Structural Control and Health Monitoring* 2017; **24**(3):n/a–n/a, doi:10.1002/stc.1887. URL http://dx.doi.org/10.1002/stc.1887.
8. Smith MC. Synthesis of mechanical networks: the inerter. *IEEE Transactions on Automatic Control* Oct 2002; **47**(10):1648–1662, doi:10.1109/TAC.2002.803532.

Table VI. Results for JMA Kobe

Response	TMD with ET					TMD with TIMET								Interstory TIMET	
	I	II	III	IV	V	I-D	I-P	II-D	II-P	III-D	III-P	IV-D	IV-P	I	II
p_{d1} (mm)	10.44	10.17	9.92	9.69	8.73	9.87	9.82	9.66	9.66	9.68	9.65	9.74	9.65	8.14	7.05
p_{d2} (mm)	17.03	16.61	16.21	15.85	14.31	16.12	16.03	15.78	15.78	15.82	15.78	15.93	15.79	13.06	11.15
p_{d3} (mm)	20.95	20.45	19.99	19.56	17.73	19.87	19.74	19.43	19.43	19.51	19.46	19.66	19.50	15.88	13.37
p_{dm} (mm)	77.99	57.27	52.18	47.98	34.33	56.55	63.98	70.73	70.68	61.84	62.07	53.96	56.50		
p_{a1} (m/s^2)	14.87	13.59	12.65	11.96	10.57	12.22	12.60	11.18	11.14	11.25	10.91	11.89	11.36	8.95	9.71
p_{a2} (m/s^2)	18.94	18.47	18.04	17.62	15.90	18.02	18.09	17.91	17.91	17.72	17.67	17.61	17.49	15.91	14.76
p_{a3} (m/s^2)	26.95	26.22	25.55	24.94	22.39	25.44	25.40	25.08	25.08	25.01	24.95	25.04	24.85	21.38	17.23
p_{am} (m/s^2)	91.25	65.46	56.28	51.00	34.02	61.25	69.64	78.65	78.59	69.14	70.06	60.46	65.23		
σ_{d1} (mm)	1.96	1.78	1.65	1.54	1.24	1.66	1.79	1.41	1.41	1.50	1.48	1.60	1.63	1.14	0.96
σ_{d2} (mm)	3.09	2.82	2.61	2.44	1.97	2.62	2.83	2.22	2.22	2.36	2.34	2.54	2.58	1.80	1.51
σ_{d3} (mm)	3.74	3.41	3.16	2.96	2.40	3.17	3.42	2.68	2.68	2.87	2.85	3.09	3.14	2.17	1.82
σ_{dm} (mm)	17.26	13.36	11.00	9.38	5.71	12.38	15.56	13.69	13.64	11.48	10.87	10.26	9.96		
σ_{a1} (m/s^2)	3.30	3.09	2.92	2.77	2.26	2.94	3.12	3.00	3.00	3.00	2.99	3.04	3.06	1.90	1.82
σ_{a2} (m/s^2)	3.69	3.37	3.12	2.92	2.35	3.14	3.46	2.79	2.78	2.84	2.80	2.99	3.01	2.31	2.05
σ_{a3} (m/s^2)	4.79	4.41	4.11	3.87	3.14	4.14	4.48	3.80	3.79	3.88	3.85	4.05	4.08	2.97	2.66
σ_{am} (m/s^2)	19.29	14.65	11.88	9.98	5.63	13.37	16.84	15.26	15.20	12.48	12.02	11.15	11.15		
E_g (Ws)	57.65	60.30	60.22	58.63	47.14	63.41	69.46	61.88	61.67	60.48	58.18	58.78	56.27	62.50	64.78
E_{in} (Ws)	65.19	67.91	68.31	67.42	61.06	70.99	76.89	65.80	65.57	65.42	62.91	64.99	62.00	65.03	67.04
Ratio (%)	88.4	88.8	88.2	87.0	77.2	89.3	90.3	94.0	94.0	92.5	92.5	90.4	90.8	96.1	96.6

Table VII. Results for El Centro

Response	TMD with ET					TMD with TIMET								Interstory TIMET	
	I	II	III	IV	V	I-D	I-P	II-D	II-P	III-D	III-P	IV-D	IV-P	I	II
p_{d1} (mm)	3.47	3.19	2.97	2.77	2.42	2.85	2.71	2.66	2.66	2.77	2.77	3.06	3.09	2.22	1.82
p_{d2} (mm)	5.60	4.95	4.41	4.21	3.78	4.32	4.26	4.23	4.23	4.22	4.22	4.61	4.63	3.53	2.87
p_{d3} (mm)	7.06	6.23	5.54	5.17	4.66	5.26	5.25	5.21	5.21	5.21	5.21	5.68	5.68	4.26	3.47
p_{dm} (mm)	30.18	24.63	21.07	18.63	11.35	23.05	26.90	27.32	27.27	22.88	22.28	19.82	19.38		
p_{a1} (m/s^2)	7.08	6.74	6.45	6.19	5.20	6.30	6.03	5.89	5.89	6.33	6.32	6.71	6.67	4.71	4.01
p_{a2} (m/s^2)	6.45	6.17	5.92	5.68	4.76	5.84	5.74	5.55	5.55	5.62	5.60	5.75	5.64	4.99	4.12
p_{a3} (m/s^2)	10.86	9.84	9.02	8.33	6.71	8.64	8.08	7.60	7.61	8.32	8.28	9.00	8.76	6.67	5.93
p_{am} (m/s^2)	33.38	26.86	22.26	18.77	10.57	24.56	28.91	27.99	27.94	23.06	22.76	20.63	20.11		
σ_{d1} (mm)	0.81	0.72	0.67	0.63	0.52	0.66	0.71	0.59	0.59	0.60	0.59	0.64	0.64	0.44	0.38
σ_{d2} (mm)	1.28	1.14	1.05	0.98	0.82	1.03	1.10	0.92	0.92	0.94	0.93	1.00	1.00	0.69	0.59
σ_{d3} (mm)	1.54	1.37	1.26	1.19	0.99	1.24	1.32	1.11	1.11	1.14	1.13	1.21	1.22	0.83	0.71
σ_{dm} (mm)	6.89	5.14	4.21	3.64	2.43	4.64	5.64	5.54	5.54	4.43	4.30	3.93	3.89		
σ_{a1} (m/s^2)	1.49	1.40	1.34	1.28	1.06	1.35	1.44	1.41	1.41	1.41	1.41	1.43	1.42	1.09	0.92
σ_{a2} (m/s^2)	1.58	1.42	1.31	1.23	1.01	1.31	1.43	1.18	1.17	1.19	1.17	1.23	1.22	0.96	0.87
σ_{a3} (m/s^2)	2.05	1.86	1.73	1.64	1.34	1.73	1.86	1.63	1.63	1.65	1.64	1.71	1.70	1.30	1.13
σ_{am} (m/s^2)	8.00	5.87	4.70	3.96	2.35	5.20	6.43	5.98	5.97	4.86	4.74	4.33	4.36		
E_g (Ws)	10.28	10.05	9.73	9.45	8.10	9.97	10.65	9.42	9.42	9.29	8.99	9.00	8.57	9.12	9.37
E_{in} (Ws)	11.70	11.42	11.15	10.98	10.56	11.21	11.82	10.25	10.24	10.18	9.86	10.09	9.58	9.60	9.77
Ratio (%)	87.8	88.0	87.2	86.1	76.7	89.0	90.1	92.0	91.9	91.2	91.2	89.2	89.4	95.0	95.9

Table VIII. Results for Taft

Response	TMD with ET					TMD with TIMET								Interstory TIMET	
	I	II	III	IV	V	I-D	I-P	II-D	II-P	III-D	III-P	IV-D	IV-P	I	II
p_{d1} (mm)	1.23	1.08	1.00	0.99	0.91	1.00	1.11	1.02	1.02	1.00	1.11	1.06	1.22	0.82	0.75
p_{d2} (mm)	2.02	1.83	1.72	1.66	1.62	1.66	1.66	1.64	1.65	1.64	1.75	1.70	1.93	1.36	1.18
p_{d3} (mm)	2.57	2.34	2.22	2.15	2.12	2.15	2.14	2.13	2.14	2.04	2.15	2.13	2.37	1.74	1.52
p_{dm} (mm)	10.37	7.42	5.93	5.31	4.31	6.37	7.46	7.96	7.95	6.78	6.86	6.20	6.73		
p_{a1} (m/s^2)	3.13	2.89	2.72	2.67	2.34	2.80	3.01	3.05	3.05	2.85	2.85	2.90	3.04	2.33	2.09
p_{a2} (m/s^2)	2.61	2.32	2.18	2.15	2.15	2.31	2.59	2.55	2.54	2.17	2.14	2.13	2.39	2.24	1.93
p_{a3} (m/s^2)	4.19	3.95	3.82	3.74	3.54	3.80	3.86	3.80	3.80	3.64	3.66	3.59	3.85	3.29	2.90
p_{am} (m/s^2)	11.76	8.25	6.48	5.57	3.98	6.87	8.07	9.27	9.28	7.70	7.96	7.27	8.27		
σ_{d1} (mm)	0.41	0.37	0.34	0.32	0.26	0.33	0.33	0.32	0.32	0.32	0.32	0.34	0.34	0.24	0.20
σ_{d2} (mm)	0.64	0.57	0.53	0.49	0.41	0.51	0.51	0.49	0.49	0.49	0.50	0.52	0.54	0.38	0.31
σ_{d3} (mm)	0.78	0.69	0.64	0.60	0.50	0.62	0.62	0.59	0.59	0.60	0.60	0.64	0.66	0.46	0.38
σ_{dm} (mm)	3.62	2.68	2.16	1.84	1.15	2.36	2.77	2.80	2.79	2.28	2.22	2.05	2.05		
σ_{a1} (m/s^2)	0.90	0.85	0.81	0.77	0.63	0.81	0.83	0.88	0.88	0.87	0.87	0.87	0.88	0.72	0.49
σ_{a2} (m/s^2)	0.80	0.72	0.67	0.63	0.52	0.66	0.68	0.65	0.65	0.64	0.64	0.66	0.67	0.58	0.47
σ_{a3} (m/s^2)	1.11	1.01	0.95	0.90	0.74	0.93	0.96	0.96	0.96	0.95	0.96	0.98	0.99	0.79	0.61
σ_{am} (m/s^2)	4.14	3.01	2.39	2.00	1.15	2.61	3.06	3.13	3.12	2.55	2.54	2.30	2.39		
E_g (Ws)	2.72	2.61	2.51	2.42	2.03	2.47	2.36	2.57	2.57	2.54	2.54	2.53	2.49	2.89	2.94
E_{in} (Ws)	3.12	3.00	2.90	2.84	2.67	2.82	2.67	2.82	2.83	2.82	2.81	2.86	2.80	3.06	3.06
Ratio (%)	87.0	87.1	86.4	85.2	76.0	87.6	88.1	90.9	90.9	90.3	90.4	88.6	89.1	94.3	96.2

9. Wang FC, Hong MF, Lin TC. Designing and testing a hydraulic inerter. *Proceedings of the Institution of Mechanical Engineers, Part C: Journal of Mechanical Engineering Science* 2011; **225**(1):66–72, doi:10.1243/09544062JMES2199.

10. Saitoh M. On the performance of gyro-mass devices for displacement mitigation in base isolation systems. *Structural Control and Health Monitoring* 2012; **19**(2):246–259, doi:10.1002/stc.419. URL http://dx.doi.org/10.1002/stc.419.

11. Watanabe Y, Ikago K, Inoue N, Kida H, Nakaminami S, Tanaka H, Sugimura Y, Saito K. Full-scale dynamic tests and analytical verification of a force-restricted tuned viscous mass damper. *Proceedings of the 15th World Conference on Earthquake Engineering*, Lisbon, Portugal, 2012.

12. Ikago K, Sugimura Y, Saito K, Inoue N. Modal response characteristics of a multiple-degree-of-freedom structure incorporated with tuned viscous mass dampers. *Journal of Asian Architecture and Building Engineering* 2012; **11**(2):375–382, doi:10.3130/jaabe.11.375.

13. Asai T, Ikago K, Araki Y. Outrigger tuned viscous mass damping system for high-rise buildings subject to earthquake loadings. *6AESE/11ANCRiSST Joint Conference*, Urbana, IL, 2015.

14. Scruggs J, Iwan W. Structural control with regenerative force actuation networks. *J. Struct. Contr. Health Monit.* 2005; **12**:24–45.

15. Cassidy I, Scruggs J, Behrens S, Gavin HP. Design and experimental characterization of an electromagnetic transducer for large-scale vibratory energy harvesting applications. *Journal of Intelligent Material Systems and Structures* 2011; doi:10.1177/1045389X11421824.

16. Asai T, Scruggs JT. Nonlinear stochastic control of self-powered variable-damping vibration control systems. *2016 American Control Conference (ACC)*, Boston, MA, 2016; 442–448, doi:10.1109/ACC.2016.7524954.

17. Asai T, Araki Y, Ikago K. Energy harvesting potential of tuned inertial mass electromagnetic transducers. *Mechanical Systems and Signal Processing* 2017; **84, Part A**:659 – 672, doi:http://dx.doi.org/10.1016/j.ymssp.2016.07.048. URL http://www.sciencedirect.com/science/article/pii/S0888327016302746.

18. Garrido H, Curadelli O, Ambrosini D. Improvement of tuned mass damper by using rotational inertia through tuned viscous mass damper. *Engineering Structures* 2013; **56**:2149 – 2153, doi:http://dx.doi.org/10.1016/j.engstruct.2013.08.044. URL http://www.sciencedirect.com/science/article/pii/S0141029613004112.

19. Cassidy IL, Scruggs JT. Nonlinear stochastic controllers for power-flow-constrained vibratory energy harvesters. *Journal of Sound and Vibration* 2013; **332**(13):3134 – 3147.

20. Cassidy IL, Scruggs JT. Statistically linearized optimal control of an electromagnetic vibratory energy harvester. *Smart Materials and Structures* 2012; **21**(8):085 003. URL http://stacks.iop.org/0964-1726/21/i=8/a=085003.

21. Scruggs JT. Multi-objective optimization of regenerative damping systems in vibrating structures. *2007 American Control Conference*, New York, NY, 2007; 2672–2677, doi:10.1109/ACC.2007.4282730.

22. Lin Y, Yong Y. Evolutionary kanai-tajimi earthquake models. *Journal of engineering mechanics* 1987; **113**(8):1119–1137.

23. Dorato P, Abdallah C, Cerone V. *Linear Quadratic Control: An Introduction*. Krieger Publishing Company: Malabar, FL, 1995.

24. de Oliveira MC, Camino JF, Skelton RE. A convexifying algorithm for the design of structured linear controllers. *Decision and Control, 2000. Proceedings of the 39th IEEE Conference on*, vol. 3, 2000; 2781–2786, doi:10.1109/CDC.2000.914229.

25. Shimomura T, Fujii T. Multiobjective control design via successive over-bounding of quadratic terms. *Decision and Control, 2000. Proceedings of the 39th IEEE Conference on*, vol. 3, 2000; 2763–2768, doi:10.1109/CDC.2000.914226.

26. Warner EC, Scruggs JT. Control of vibratory networks with passive and regenerative systems. *American Control Conference (ACC), 2015*, Chicago, IL, 2015; 5502–5508, doi:10.1109/ACC.2015.7172200.

27. Dyke SJ, Jr BFS, Quast P. Role of control-structure interaction in protective system design. *Journal of Engineering Mechanics* Issue: object: doi:101061/jenmdt1995121issue-2, revision: rev:1479269508442-23046:doi:101061/jenmdt1995121issue-2, ; **121**(2), doi:10.1061/(ASCE)0733-9399(1995)121:2(322).

28. Scruggs JT, Iwan WD. Structural control with regenerative force actuation networks. *Structural Control and Health Monitoring* 2005; **12**(1):25–45, doi:10.1002/stc.50. URL http://dx.doi.org/10.1002/stc.50.

29. Scruggs JT, Iwan WD. Optimal nonlocal and asymmetric structural damping using regenerative force actuation networks. *Journal of Engineering Mechanics* Issue: object: doi:101061/jenmdt2006132issue-9, revision: rev:1479273067672-25181:doi:101061/jenmdt2006132issue-9, ; **132**(9), doi:10.1061/(ASCE)0733-9399(2006)132:9(932).

30. Asai T, Spencer BF, Iemura H, Chang CM. Nature of seismic control force in acceleration feedback. *Structural Control and Health Monitoring* 2013; **20**(5):789–803, doi:10.1002/stc.1496. URL http://dx.doi.org/10.1002/stc.1496.

31. Housner W, Jennings PC. Generation of artificial earthquakes. *Journal of the Engineering Mechanics Division* 1964; **90**(1):113–150.

32. Spencer BF, Dyke SJ, Deoskar HS. Benchmark problems in structural control: part i—active mass driver system. *Earthquake Engineering & Structural Dynamics* 1998; **27**(11):1127–1139, doi:10.1002/(SICI)1096-9845(1998110)27:11⟨1127::AID-EQE774⟩3.0.CO;2-F.

33. Chopra A. *Dynamics of Structures: Theory and Applications to Earthquake Engineering*. Prentice Hall International Series in Civil Engineering And, Pearson/Prentice Hall: Upper Saddle River, NJ, 2007. URL https://books.google.co.jp/books?id=jce0QgAACAAJ.